Site-Directed Conversion of Cysteine-565 to Serine in PsaB of Photosystem I Results in the Assembly of [3Fe-4S] and [4Fe-4S] Clusters in F_X. A Mixed-Ligand [4Fe-4S] Cluster Is Capable of Electron Transfer to F_A and F_B[†]

Patrick V. Warren,[‡] Lawrence B. Smart,[§,∥] Lee McIntosh,[§] and John H. Golbeck*[,‡]

Department of Biochemistry, University of Nebraska, Lincoln, Nebraska 68583-0718, and Department of Biochemistry and Department of Energy Plant Research Laboratory, Michigan State University, East Lansing, Michigan 48824

Received December 11, 1992; Revised Manuscript Received January 19, 1993

ABSTRACT: We reported earlier [Smart, L. B., Warren, P. V., Golbeck, J. H., & McIntosh, L. (1993) *Proc. Natl. Acad. Sci. U.S.A. 90*, 1132–1136] that the site-directed conversion of cysteine-565 to serine (C565S) in PsaB of *Synechocystis* sp. PCC 6803 leads to an accumulation of photosystem I polypeptides and the low-temperature photoreduction of the terminal electron acceptors F_A and F_B. In this paper, we report the occurrence of a $[3Fe\text{-}4S]^{1+,0}$ cluster in dodecyl maltoside-solubilized photosystem I complexes prepared from the C565S mutant. The [3Fe-4S] cluster is reducible with dithionite at pH 6.5, implying a midpoint potential considerably more oxidizing than either F_A or F_B. Similar to the behavior of F_X, the [3Fe-4S] cluster undergoes partial, reversible photoreduction when the complex is illuminated at 15 K, and complete photoreduction when the sample is illuminated during freezing. Contrary to the result expected in the presence of a relatively high-potential F_X, there is significant low-temperature and room temperature photoreduction of F_A and F_B in the C565S complex. Although the F_A and F_B resonances are more intense when the complex is frozen during illumination, they still account for <60% of F_A and F_B found by chemical reduction. When the F_A and F_B clusters are prereduced with dithionite at pH 10.0, a new set of resonances appear upon illumination at $g = 2.015$, 1.941, and 1.811, and disappear on subsequent darkness. The species giving rise to this signal is most likely a mixed-ligand $[4Fe\text{-}4S]^{2+,1+}$ cluster located in the F_X site. This acceptor, denoted F_X', has different ESR properties from wild-type F_X, but it has a redox potential low enough to transfer an electron to F_A and F_B. We suggest that F_X' is assembled as a functional [4Fe-4S] cluster in vivo but in a minority of centers F_X' loses an iron, resulting in a population of [3Fe-4S] clusters which cannot pass the electron forward to F_A or F_B. The redox behavior of the [3Fe-4S] and mixed-ligand [4Fe-4S] clusters is consistent with the participation of F_X in electron transfer from A_1^- to F_A and F_B.

The function of the photosystem I (PSI)[1] reaction center is to transform the energy of a photon into stable chemical free energy in the form of reduced NADPH [reviewed in Bryant (1992) and Golbeck (1992)]. Photosystem I also functions to cycle an electron through the cytochrome b_6/f complex so that one or more protons can be translocated for the purpose of supplying additional ATP. Both of these tasks are accomplished in a specialized reaction center which contains ~100 chlorophyll (chl) *a* antenna molecules, a specialized chl dimer to trap the exciton, and a specialized chl monomer to function as a primary electron acceptor. The charge separation between these donor/acceptor chl molecules is short-lived, and must be stabilized by a series of secondary acceptors which serve to transfer the electron away from the primary acceptor before the charge recombination can occur. In photosystem I, the electron-acceptor chain consists of a molecule of phylloquinone (or 5′-hydroxyphylloquinone), an interpolypeptide [4Fe-4S] cluster, F_X (both located on the PsaA/PsaB heterodimer), and two [4Fe-4S] clusters, F_A/F_B (located on an extrinsic stromal protein, PsaC). It is widely assumed, although not rigorously proven, that the electron passes sequentially from A_0- through A_1 and F_X to the terminal iron–sulfur clusters F_A and F_B.

The F_X cluster is considered to be a rare instance of an interpolypeptide [4Fe-4S] cluster, where two of the cysteine ligands are provided by PsaA and the other two cysteine ligands are provided by PsaB (Golbeck & Cornelius, 1986). The other known instance of an interpolypeptide [4Fe-4S] cluster occurs in the Fe protein in nitrogenase, where the cluster is ligated by two cysteines on each of two identical 30-kDa subunits (Hausinger & Howard, 1983; Georgiadis et al., 1992). F_X may occupy the same relative position as the non-heme iron in the purple bacterial reaction center and in photosystem II, but it may have a different function. Unlike the non-heme iron, the F_X acceptor is thought to undergo redox chemistry under physiologically-relevant conditions. Its role in photosystem I may be to divert the electron out of the membrane phase and into the stromal phase, ultimately reducing soluble ferredoxin through the involvement of bound F_A and F_B. The midpoint potential of the F_X^-/F_X couple is –705 mV (Chamorovsky & Cammack, 1982), which is appropriate for an electron carrier located between the intermediate electron acceptor A_1 [E_m, –800 mV (Sétif & Bottin, 1989)] and the terminal F_A/F_B clusters [E_m, –530/–580 mV (Evans & Heathcote, 1980)]. The ESR spectrum of F_X is broad, the

[†] Published as Journal Series No. 10203 of the University of Nebraska Agricultural Research Division. Supported by grants from the National Science Foundation (MCB-9205756 to J.H.G.), the U.S. Department of Energy (DE-FG02-90-ER20021 to L.M.), and MSU/REF (to L.M.).

* Correspondence should be addressed to this author. Telephone: (402) 472-2931. Telefax: (402) 472-7842.

[‡] University of Nebraska.

[§] Michigan State University.

[∥] Present address: Department of Vegetable Crops, Mann Laboratory, University of California, Davis, CA 95616.

[1] Abbreviations: chl, chlorophyll; PSI, photosystem I; ESR, electron spin resonance; DCPIP, dichlorophenolindophenol; NADPH, reduced nicotinamide adenine dinucleotide phosphate; ATP, adenosine 5′-triphosphate; CW, continuous wave; DM, dodecyl maltoside; FPLC, fast protein liquid chromatography.

0006-2960/93/0432-4411$04.00/0

average g-value is closer to 1.90 than 1.94, and the low-temperature optimum and high $P^{1/2}$ reflect an unusually rapid spin relaxation mechanism (Evans et al., 1976). Subtle changes produced by the protein geometry of interpolypeptide clusters may give rise to the mixed $S = {}^1/_2$ and ${}^3/_2$ spin states of the Fe protein in nitrogenase and the enhanced spin relaxation properties of F_X.

In spite of its pivotal location in photosystem I, there is only limited experimental evidence to support a role for F_X in forward electron flow. There are only two reports on the kinetic properties of F_X (Crowder & Bearden, 1983; Sétif et al., 1984), both of which indicate that at low temperature there is little kinetic opportunity for an additional electron acceptor operating between A_1 and F_A. Direct kinetic measurements are difficult to make, since the nearly identical optical spectra of F_X, F_B, and F_A preclude measurement of forward electron-transfer rates between the three iron–sulfur clusters. The low-temperature ESR spectra of F_X, F_B, and F_A are distinct, but the electron-transfer rates between the clusters are faster than the rise time of a conventional CW spectrometer (Shuvalov et al., 1979).

Because of these problems, we adopted a different strategy to investigate the role of F_X in forward electron flow. It was recently shown that substitution of cysteine by serine results in the assembly of a [3Fe-4S] cluster in the 4[4Fe-4S] protein dimethyl-sulfoxide reductase (Rothery & Weiner, 1991). Since the midpoint potential of a [3Fe-4S] cluster is typically higher than that of a [4Fe-4S] cluster (Beinert & Thomson, 1983), the incorporation of a [3Fe-4S] cluster in F_X could allow us to test its participation for forward electron flow. We have demonstrated that the substitution of a serine for a cysteine in PsaB of *Synechocystis* sp. PCC 6803 leads to the accumulation of photosystem I polypeptides and low-temperature photoreduction of F_A and F_B (Smart et al., 1993). Here we present evidence that PSI complexes from the C565S mutant contain a [4Fe-4S] cluster in the F_X site. This mixed-ligand [4Fe-4S] cluster has altered ESR properties but is nevertheless capable of reducing F_A and F_B at 15 K. We also find a population of [3Fe-4S] clusters in the F_X site that may result from the loss of an iron atom from the mixed-ligand [4Fe-4S] cluster. The high redox potential of the [3Fe-4S] cluster renders it incapable of reducing F_A or F_B.

MATERIALS AND METHODS

Photosystem I Subthylakoid Preparations. A fully segregated mutant of the cyanobacterium *Synechocystis* sp. PCC 6803 was produced with a site-directed change in the *psaB* gene causing the amino acid substitution of cysteine to serine at position 565 (Smart et al., 1993). Cells were grown under light-activated heterotrophic growth conditions (Anderson & McIntosh, 1991) in carboys with 15 L of BG-11 medium supplemented with 5 mM glucose. After being harvested with a continuous-flow rotor (DuPont Sorvall, Wilmington, DE), the cells were stored in BG-11 with 15% v/v glycerol at −80 °C. In the case of C565S, the medium was supplemented with spectinomycin (20 mg/L; Sigma Chemical Co., St. Louis, MO). Thylakoid membranes were isolated using the procedure described in Smart et al. (1991). The cells were broken in buffer containing 20 mM MES (4-morpholineethanesulfonic acid), pH 6.5, 0.8 M sucrose, and proteinase inhibitors using a Bead Beater (Biospec Products, Bartelsville, OK). Membranes were precipitated with 20 mM $CaCl_2$ and 5% PEG-8000 and were pelleted by centrifugation. Dodecyl maltoside (DM)–photosystem I complexes were prepared using a described protocol (Norem et al., 1991). Membranes were solubilized in 1% DM (Anatrace, Inc., Maumee, OH) followed by ion-exchange chromatography over Fast Flow Q Sepharose (Pharmacia, Piscataway, NJ). Fractions with absorption maxima greater than 676 nm were pooled, and photosystem complexes were precipitated using 15% PEG-3400 (Fluka Chemical Co., Ronkonkoma, NY) and pelleted by centrifugation. Photosystem complexes in this pellet were resuspended in buffer with DM and were fractionated by FPLC over a Mono Q column (Pharmacia). Fractions with absorption maxima greater than 678 nm were pooled, and PSI complexes were precipitated using 15% PEG-3400 and pelleted by centrifugation. The PSI complexes in this pellet were resuspended in buffer containing 50 mM Tris, pH 8.3, and 25% glycerol and were used for subsequent analysis.

Electron Spin Resonance Spectroscopy. Electron spin resonance (ESR) studies were performed with a Bruker ECS-106 X-band spectrometer. Cryogenic temperatures were maintained with an Oxford liquid helium cryostat and an Oxford ITC4 temperature controller. Microwave frequency was sampled during run-time with a Hewlett-Packard 5340A frequency counter. The field was calibrated using the position of the $g = 2.0025$ resonance derived from the $P700^+$ cation. Sample temperatures were monitored by a calibrated thermocouple situated beneath the 3-mm i.d. quartz sample tube and referenced to liquid nitrogen. Actinic illumination of the sample was provided by a 150-W xenon arc source (Oriel) filtered through 5 cm of water and passed through a heat-absorbing filter to remove the near-IR wavelengths. All samples contained 500 μg/mL chl, 1 mM sodium ascorbate, and 30 μM DCPIP in 50 mM Tris-HCl, pH 8.3. Chemically-reduced samples contained excess dithionite in 0.1 M glycine, pH 10.0.

Flash-Induced Absorption Changes. Flash-induced absorption changes in the microsecond time range were determined between 720 and 830 nm with a laboratory-built double-beam spectrometer (Warren et al., 1993). The measuring beam was provided by a CW titanium–sapphire laser (Schwartz ElectroOptics, Orlando, FL), pumped by a 5-W argon-ion laser (Spectra Physics Model 2020-05). Due to instability in the argon-ion laser, the measuring beam was split; one beam was passed through the sample, and the other passed directly to a pair of PIN-10D photodiodes. The photocurrents were converted to a voltage with a 100-Ω resistor, and the signals were amplified and subtracted using a DC-coupled differential comparator (Tektronix Model 11A33) and digitized with a Tektronix DSA 601 oscilloscope. Curve fitting and data analysis were performed using IGOR (Wavemetrics, OR) on a Macintosh IIci computer. The excitation beam was provided by a 2.3-MW nitrogen laser (PTI, London, ON), operating at a frequency of 1 Hz. All samples contained 100 μg/mL chl, 0.1 mM DCPIP, and 5 mM sodium ascorbate in 100 mM Tris-HCl, pH 8.3.

RESULTS

ESR Spectral Characterization of a [3Fe-4S] Cluster in the C565S Mutant. The low-temperature ESR spectrum of a dodecyl maltoside–photosystem I complex (DM–PSI) prepared from the C565S mutant of *Synechocystis* sp. PCC 6803 is shown in Figure 1. The most prominent feature in the dark spectrum is the appearance of a set of resonances at $g = 2.018$, 2.001, and 1.991 (Figure 1A). These resonances are characteristic of $[3Fe\text{-}4S]^{1+,0}$ clusters which, under oxidizing conditions, typically show a rhombic ESR spectrum with $g_z = 2.02$, $g_y = 2.00$, and $g_x = 1.97$ (Beinert & Thomson, 1983; Huynh et al., 1980). When the DM–PSI sample is illuminated at 15 K, the narrow $P700^+$ radical appears at g

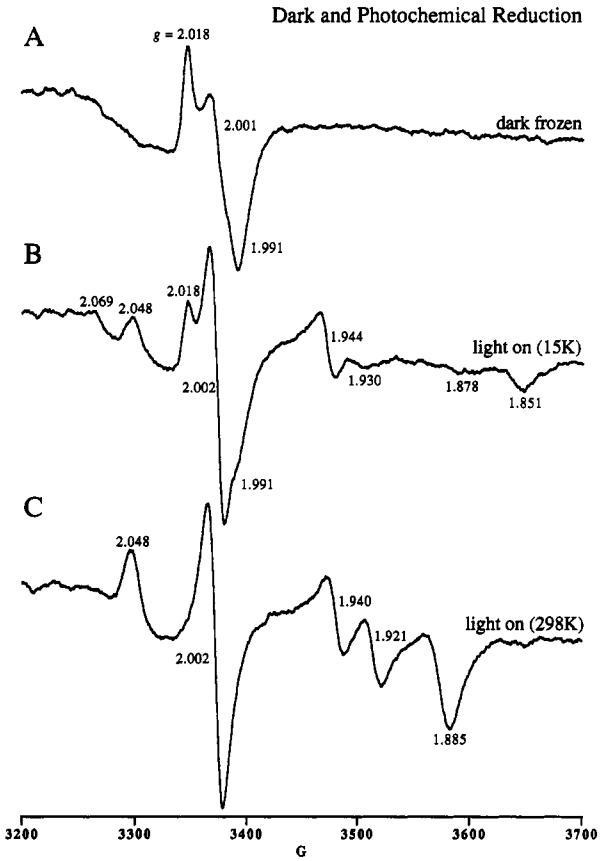

FIGURE 1: ESR spectra of the C565S DM–photosystem I complex in the presence of 1 mM sodium ascorbate and 30 μM DCPIP in 50 mM Tris-HCl, pH 8.3. (A) Spectrum after freezing the sample in darkness; (B) spectrum after freezing the sample in darkness and illumination at 15 K; (C) spectrum after freezing the sample during illumination. The resonances at $g = 2.018$ and 1.991 were the same intensity in a sample frozen in darkness without added ascorbate and DCPIP. Spectrometer conditions: temperature, 15 K; microwave power, 20 mW; microwave frequency, 9.128 GHz; receiver gain, 2.0×10^4; modulation amplitude, 10 G at 100 kHz; magnetic field, 3450 G with a scan width of 500 G. All spectra were taken at 500 μg/mL chl.

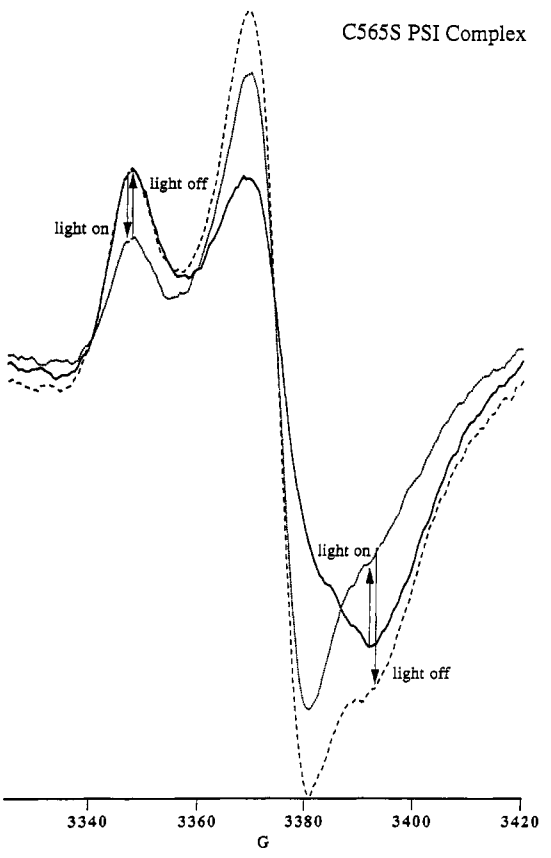

FIGURE 2: ESR spectra of the C565S DM–photosystem I complex showing the effect of illumination in the region around $g = 2.00$. The sample was frozen in darkness (solid line), illuminated with a 150-W xenon lamp during the 3-min period of measurement (dotted line), and measured in subsequent darkness (dashed line). The temperature of the sample rose less than 1 K on illumination. Spectrometer conditions are the same as in Figure 1 except that the magnetic field was centered at 3370 G with a scan width of 100 G.

= 2.002, and the resonances at $g = 2.018$ and 1.991 partially disappear (Figure 1B). These changes are more clearly shown in Figure 2, which depicts only 100 G of the $g = 2$ region of the spectrum. In addition to a strong midfield derivative resonance at $g = 2.001$, the dark spectrum (solid line) shows the $g = 2.018$ and 1.991 resonances characteristic of a $[3Fe\text{-}4S]^{1+}$ cluster. When the sample is illuminated (dotted line), about half of the spins represented by the $g = 2.018$ and 1.991 species disappear due to reduction of the $[3Fe\text{-}4S]^{1+}$ cluster to the ESR-silent $[3Fe\text{-}4S]^0$ state, and an intense resonance appears at $g = 2.002$ due to oxidation of P700 to $P700^+$. When the light is turned off (Figure 2, dashed line), the resonance at $g = 2.018$ reappears, signaling complete reoxidation of the $[3Fe\text{-}4S]^0$ cluster to the $[3Fe\text{-}4S]^{1+}$ oxidation state. In contrast, the low-temperature ESR spectrum of untreated thylakoid membranes isolated from the C565S mutant of *Synechocystis* sp. PCC 6803 shows no appreciable signals in the dark (data not shown). The ability to undergo reversible photoreduction is a property inherent to the F_X cluster; the F_A and F_B clusters undergo irreversible photoreduction at cryogenic temperatures. The larger signal at $g = 2.002$ in subsequent darkness is due not only to the recovery of the midfield resonance of the $[3Fe\text{-}4S]^{1+}$ cluster but also to a population of $P700^+$ that remains irreversibly photooxidized. This irreversibility indicates that a portion of P700 transfers its electron beyond F_X, most likely to F_A and F_B. On the basis of the relative number of spins involved, between one-third and one-half of P700 is paired with the reversible photoreduction of the [3Fe-4S] cluster, and the remaining P700 is paired with the irreversible photoreduction of a more distant electron acceptor.

A scan at a field width of 500 G shows that this distant electron acceptor is indeed F_A and F_B. The irreversible photoreduction of F_A is shown by the resonances at $g = 2.048$, 1.944, and 1.851, and that of F_B at $g = 2.069$, 1.930, and 1.878, and the 5:1 ratio of F_A to F_B (Figure 1B) is similar to that observed in wild-type DM–PSI complexes (not shown). When the sample is frozen during illumination (Figure 1C), the low-field and high-field resonances of F_A and F_B merge at $g = 2.048$ and 1.885, and the midfield resonances of F_A at $g = 1.940$ and of F_B at $g = 1.921$ remain distinct. This is normal behavior, and indicates that the magnetic interaction between the F_A and F_B clusters is unaffected by the C565S change in PsaB. Because of the interaction between F_A and F_B, it is difficult to quantify the number of spins involved, but the sum of F_A plus F_B reduced by illumination at 15 K is about 60% of that found when the sample is illuminated during freezing. This is the same efficiency of F_A and F_B photoreduction observed in wild-type DM–PSI complexes at 15 K. This relative inefficiency is observed only at low temperatures and is probably due to the failure of a population of A_1- to transfer its electron to F_X (Sétif et al., 1984). The effect is more clearly observed in a P700–F_X core, where only ~50% of the F_X cluster can be photoreduced at 15 K relative to that which can be photoaccumulated by freezing during illumination (Parrett et al., 1989). Although the reversible

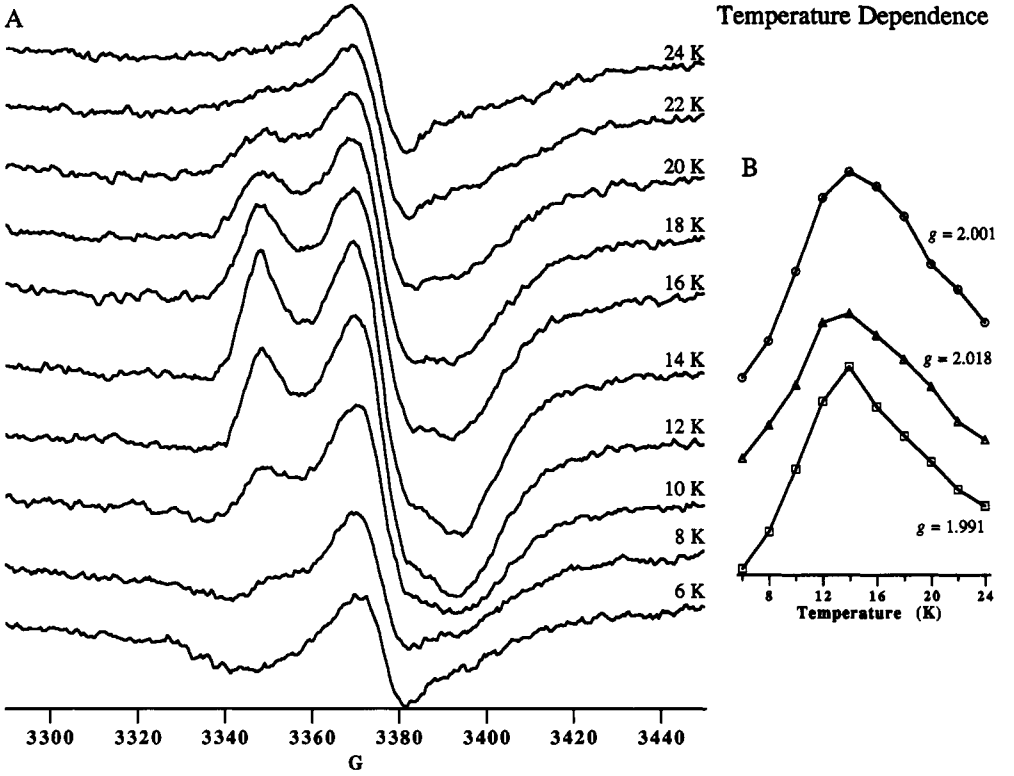

FIGURE 3: Effect of temperature on the intensity of the g = 2.018, 2.001, and 1.991 resonances in a dark-adapted sample of a C565S DM–photosystem I complex. (A) Spectra were recorded every 2 K from 6 K to 24 K. (B) Plot of intensity of the g = 2.018 (low-field), 2.001 (midfield), and 1.991 (high-field) resonances vs temperature. Sample conditions and spectrometer conditions are the same as in Figure 1 except that the field was scanned from 3250 to 3450 G and the microwave power was 20 mW.

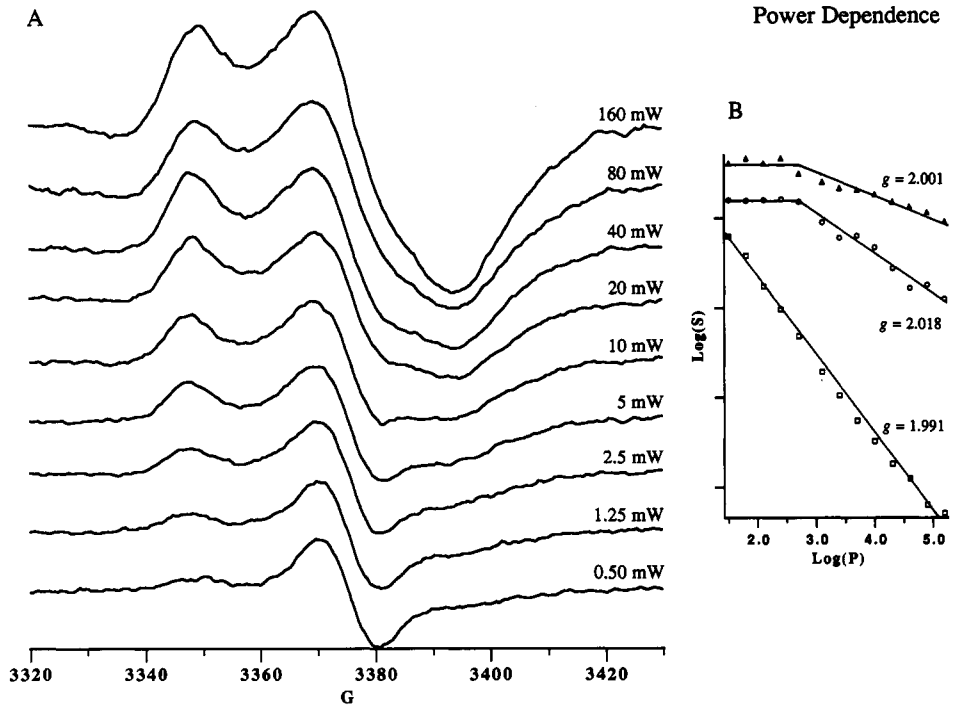

FIGURE 4: Effect of microwave power on the intensity of the g = 2.018, 2.001, and 1.991 resonances in a dark-adapted sample of a C565S DM–photosystem I complex. (A) Spectra were recorded from 38 dB of attenuation (32 μW) to 1 dB (160 mW); only 0.5–160 mW is shown. (B) Plot of $\log(I/P^{1/2})$ of the g = 2.018 (low-field), 2.001 (midfield), and 1.991 (high-field) resonances vs $\log P$. The Y-scale is offset arbitrarily. Sample conditions and spectrometer conditions are the same as in Figure 1 except that the field was scanned from 3320 to 3430 G and the temperature was 14 K.

component of $P700^+$ photooxidation is paired with the reversible photoreduction of the [3Fe-4S] cluster in the C565S mutant, about half of the available clusters appear to be capable of accepting an electron at 15 K. Unlike wild-type F_X, the $[3Fe\text{-}4S]^0$ F_X cluster cannot transfer its electron forward to F_A or F_B; this, and the relative inefficiency in A_1 forward electron transfer, leads to the partial photoreduction of the [3Fe-4S] cluster in the light.

The effect of temperature on the intensity of the $[3Fe\text{-}4S]^{1+}$ signal is shown in Figure 3A. The g = 2.018 and 1.998 resonances are observed only over a narrow temperature range of 10–20 K, with an optimum of 14 K. The midfield resonance

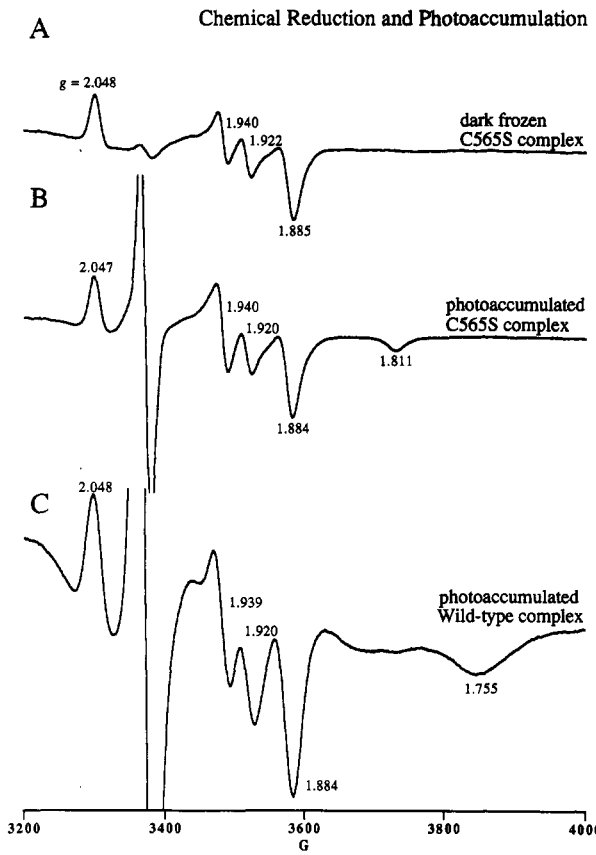

FIGURE 5: ESR spectra of the C565S DM–PSI and wild-type–photosystem I complexes in the presence of excess dithionite in 0.1 M glycine, pH 10.0. (A) Spectrum after freezing the C565S complex in darkness; (B) spectrum after freezing the C565S complex during illumination to photoaccumulate reduced electron acceptors; (C) spectrum after freezing the wild-type complex during illumination to photoaccumulate reduced electron acceptors. Spectrometer conditions: microwave power, 40 mW; microwave frequency, 9.128 GHz; receiver gain, 2.0×10^4; modulation amplitude, 32 G at 100 kHz; magnetic field, 3600 G with a scan width of 800 G. The temperature was 15 K in (A) and (B) and 8 K in (C). All spectra were taken at 500 μg/mL chl.

at $g = 2.001$ remains nearly the same intensity at temperatures ranging from 6 to 24 K (Figure 3B), indicating that a significant fraction of the signal may be derived from a different paramagnetic center. This conclusion is borne out by a study of the signal intensity as a function of microwave power. As shown in Figure 4A, the intensity of the $g = 2.018$ and 1.991 resonances increases with power to a maximum of 160 mW (1 dB). In contrast, the midfield resonance observed at a magnetic field between 3365 and 3375 G does not appear much larger at 160 mW (1 dB) than at 0.5 mW (26 dB). The effect of microwave power is best seen in Figure 4B by plotting the $\log(I/P^{1/2})$ vs $\log P$ (where I is the signal intensity and P is the microwave power). The $P^{1/2}$ of the [3Fe-4S] cluster represented by the $g = 2.018$ and 1.991 resonances is 15 mW, compared to <5 mW for the species represented by the $g = 2.001$ resonance. We conclude that a portion of the midfield resonance is derived from a paramagnetic species distinct from the $[3Fe\text{-}4S]^{1+}$ cluster.

ESR Spectral Characterization of a Mixed-Ligand [4Fe-4S] Cluster in the C565S Mutant. The irreversible photooxidation of $P700^+$ and the irreversible photoreduction of F_A and F_B indicate either that there is a functional iron–sulfur cluster present in the F_X site or that F_X is not required for forward electron flow from A_1 to F_A and F_B. As indicated above, about one-third to one-half of P700 is able to photochemically reduce the F_A/F_B clusters. One consequence

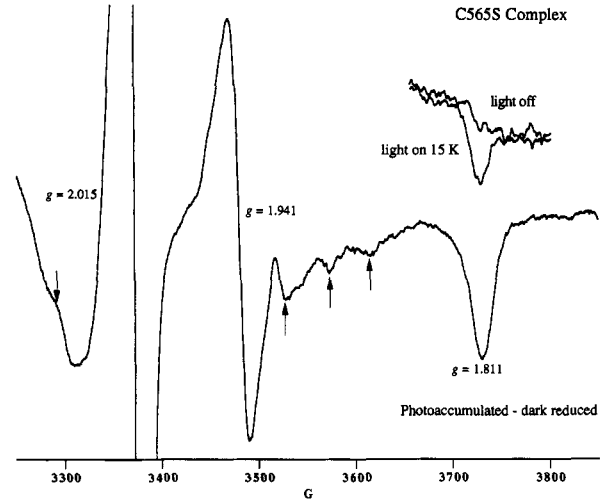

FIGURE 6: Light-minus-dark difference spectrum of the C565S DM–PSI complex obtained by subtracting the dark-reduced sample (Figure 5A) from the dark-reduced, photoaccumulated sample (Figure 5B). The minor resonances at 3275, 3520, 3575, and 3615 G are subtraction artifacts from the reduced F_A and F_B clusters where the g-values of the resonances have changed slightly due to interaction, probably with F_X' (see text). Spectrometer conditions identical to Figure 5. Inset: the effect of illumination on the C565S DM–PSI complex frozen in darkness. The spectrum shows the reversibility of the $g = 1.811$ resonance after two light–dark cycles of light-on at 15 K and light-off after light-on. Conditions are identical to Figure 5A above.

of this stoichiometry is that only one-half to two-thirds of the total population of F_A and F_B should be reducible photochemically. Figure 5A shows that F_A and F_B can be chemically reduced in the C565S DM–PSI complex with sodium dithionite at pH 10.0; the number of spins represented is about twice that which can be observed by photoaccumulating F_{A^-} and F_{B^-} (data not shown; Figures 1C and 5A are not comparable due to different conditions). There is no indication of the dark reduction of a third iron–sulfur cluster representative of F_X. When the same sample is illuminated during freezing to photoaccumulate the electron acceptor system, the $g = 2.047$, 1.920, and 1.884 resonances of F_A and F_B remain unaffected, but the $g = 1.940$ resonance increases in intensity and a new signal appears at $g = 1.811$ (Figure 5B). The latter resonance has not been observed previously in photosystem I complexes. In contrast, when a wild-type DM–PSI complex is chemically reduced with dithionite and frozen during illumination (Figure 5C), the broad high-field resonance of F_{X^-} appears at $g = 1.755$ (the $g = 1.87$ midfield and $g = 2.04$ low-field resonances underly the sharper resonances of F_A and F_B).

The difference spectrum between the photoaccumulated and dark-frozen spectra of the C565S DM–PSI complex (Figure 6) reveals a rhombic set of resonances with g-values of 2.015 (the low-field peak is most likely the shoulder near the large radical at $g = 2.002$), 1.941, and 1.811. This spectrum does not appear on chemical reduction with dithionite at pH 10.0; hence, the midpoint potential of the species which gives rise to this set of resonances is less than –600 mV. Reminiscent of the behavior of F_X, the $g = 2.015$, 1.941, and 1.811 resonances are observed only when F_A and F_B are prereduced prior to illumination. We shall henceforth denote this acceptor as F_X' to distinguish it from wild-type F_X. The weaker resonances in Figure 6 (depicted by arrows) are subtraction artifacts, probably arising from magnetic interaction of reduced F_X' with F_{A^-} and F_{B^-}, and having the effect of altering slightly the g-values of the latter resonances. When the C565S DM–PSI complex is frozen in darkness in the presence of prereduced F_A and F_B, the $g = 1.811$ resonance of reduced F_X' appears on illumination at 15 K, and disappears

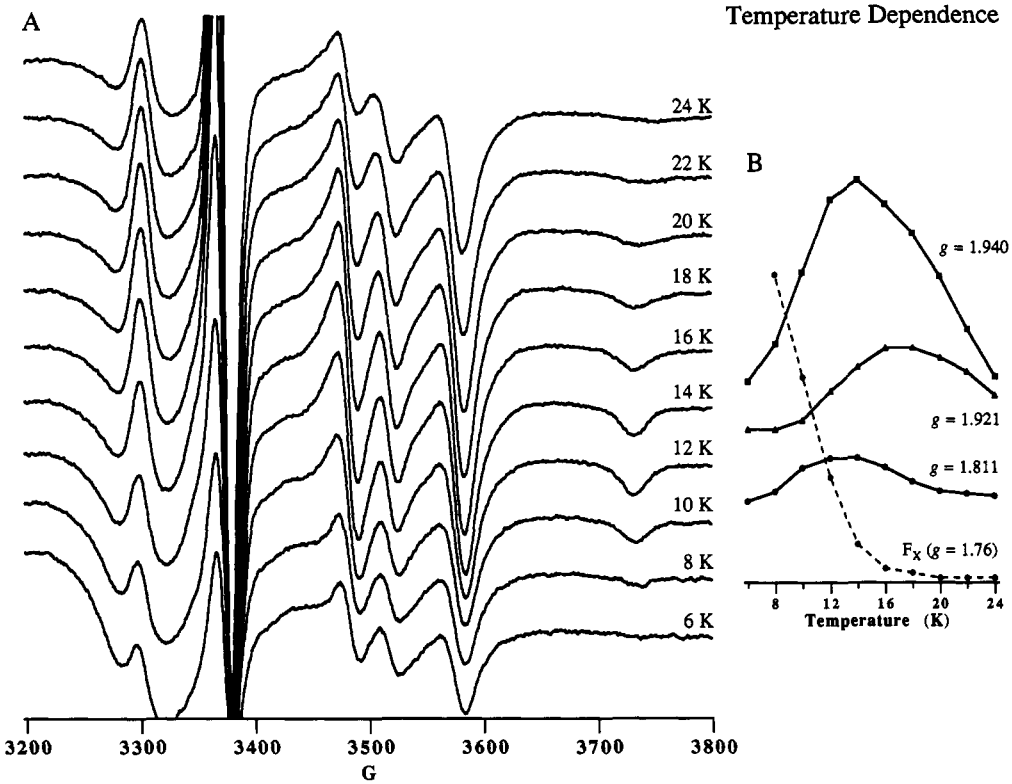

FIGURE 7: Effect of temperature on the intensity of iron–sulfur centers F_A at $g = 1.940$ ($g = 1.940$ also contains some contribution from F_X'), F_B at $g = 1.921$, and F_X' at $g = 1.811$ in a photoaccumulated sample of the C565S DM–photosystem I complex. (A) Spectra were recorded every 2 K from 6 K to 24 K. (B) Plot of the intensity of the $g = 1.940$ resonance from superimposed F_X' and F_A, the $g = 1.921$ resonance from F_B, and the $g = 1.811$ resonance from F_X' in the C565S complex. The $g = 1.76$ resonance from F_X in a wild-type–PSI complex is shown for reference. Sample conditions and spectrometer conditions are the same as in Figure 6 except that the field was scanned from 3200 to 3800 G and the microwave power was 40 mW.

on subsequent darkness (Figure 6, inset). The reason for the partial photoreduction at 15 K is probably the same inefficiency of A_1 to transfer its electron forward at low temperature as discussed above.

The effect of temperature on signal intensity is shown in Figure 7A. The $g = 1.811$ resonance and a portion of the $g = 1.940$ resonance of F_X' are observed only over a narrow temperature range of 10–20 K. The F_A and F_B resonances at $g = 2.04$, 1.92, and 1.86 can be readily seen at temperatures ranging from 6 to 24 K. The effect of temperature is more easily seen in Figure 7B, where the signal intensity is plotted against the absolute temperature. The temperature optimum for the $g = 1.811$ resonance of F_X' of 14 K is slightly lower than the 18 K optimum for F_A and F_B. This behavior is strikingly different from that of the $[4Fe\text{-}4S]^{2+,1+}$ F_X cluster in a wild-type DM–PSI complex, which has a maximum at 8 K and very little signal intensity at 14 K. The effect of microwave power on signal intensity is shown in Figure 8A. The $g = 1.811$ resonance and a portion of the $g = 1.940$ resonance of F_X' increase with microwave power to a maximum of 160 mW (1 dB). The effect of microwave power is best seen in Figure 8B by plotting $\log(I/P^{1/2})$ vs $\log P$ (where I is the signal intensity and P is the microwave power). The $P^{1/2}$ of the F_X' cluster represented by the $g = 1.811$ resonance is 20 mW, in contrast to 90 mW for the [4Fe-4S] F_X cluster in the wild-type photosystem I complexes. On the basis of the appearance of the rhombic set of resonances at $g = 2.015$, 1.941, and 1.811 upon photoaccumulating the C565S DM–PSI complex, and on the partial reversibility of the signal when the sample is illuminated in the presence of prereduced F_A and F_B, these resonances are most probably derived from a mixed-ligand $[4Fe\text{-}4S]^{2+,1+}$ cluster located in the F_X site.

Optical Kinetic Properties of the C565S DM–PSI Complex. The flash-induced absorption change in the C565S DM–PSI complex is compared with that of a wild-type DM–PSI complex in Figure 9A,B. The initial absorption change on a single-turnover flash in the C565S DM–PSI complex is the same as the wild-type DM–PSI complex, but about 25% of the transient decays with a half-time of 10 μs. When measured on a longer time scale (not shown), the back-reaction between $P700^+$ and $[F_A/F_B]^-$ in the C565S DM–PSI complex was about 30 ms, similar to the wild-type DM–PSI complex. Given that the total absorption change on the flash represents 100% of the available P700, we calculate a ratio of ~100 chl/P700 in both the wild-type and C565S DM–PSI complexes. On the basis of the relative intensities of the ESR resonances (see Figure 5), the DM–PSI complex isolated from the C565S mutant contains ~65% of F_A and F_B compared with DM–PSI complexes isolated from wild-type thylakoids. The optical and ESR data are therefore in rough agreement.

Figure 9C shows the flash-induced difference spectrum of these preparations from 720 to 830 nm. The wild-type and C565S DM–PSI complexes show a peak at 810 and very little absorption change between 720 and 750 nm, consistent with the identification as a $P700^+$ cation and not a chlorophyll or P700 triplet (Mathis & Sétif, 1981; Warren et al., 1993). The 10-μs component in the C565S complex may result from the back-reaction of A_1^- with $P700^+$ in a population of reaction centers where forward electron transfer to F_X is prohibited because of inefficiency at room temperature or damage to F_X. The long-lived charge separation (>10 μs) indicates that on a single-turnover flash, charge separation between P700 and F_X, F_B, or F_A is efficient in 80% of the reaction centers at 298 K.

All attempts to isolate a P700–F_X core (Parrett et al., 1989) by removal of PsaC, PsaD, and PsaE using chaotropic agents failed. The dissociation of these stromal, peripheral polypeptides resulted in complete destruction of the F_X cluster and

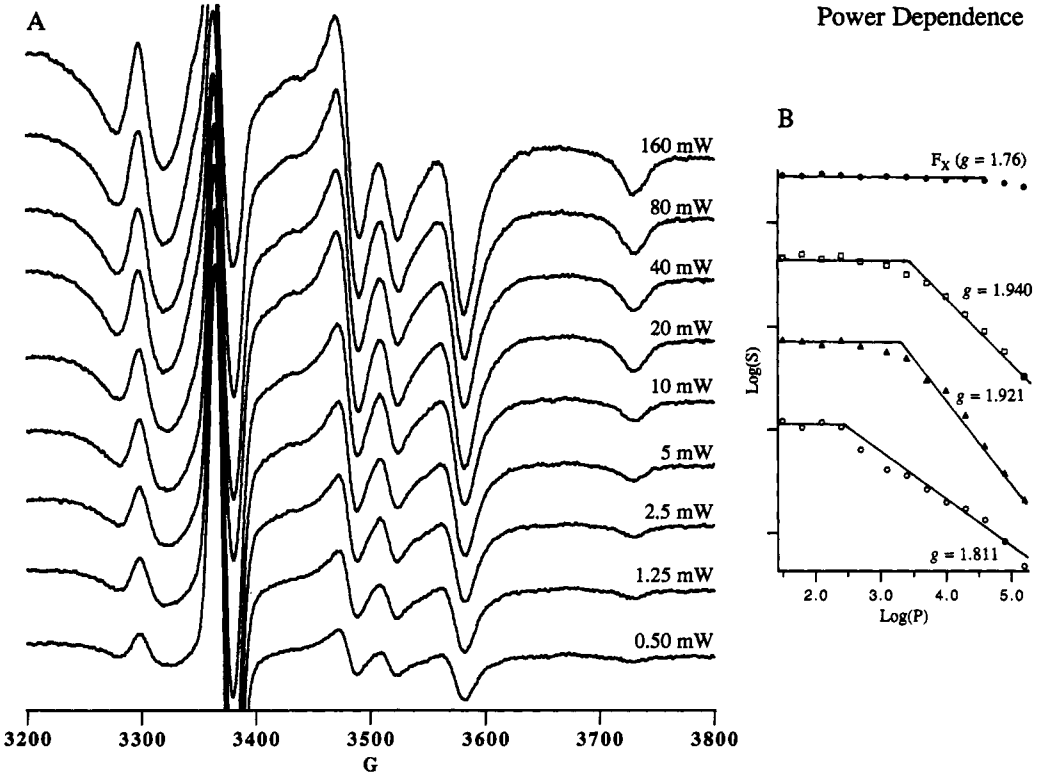

FIGURE 8: Effect of microwave power on the intensity of the F_A, F_B, and F_X' resonances in a preduced, photoaccumulated sample of the C565S DM–photosystem I complex. (A) Spectra were recorded from 38 dB of attenuation (32 μW) to 1 dB (160 mW). (B) Plot of $\log(I/P^{1/2})$ vs $\log P$ of the $g = 1.940$ resonance from superimposed F_A and F_X', the $g = 1.921$ resonance from F_B, and the $g = 1.811$ resonance from F_X' in the C565S complex. The $g = 1.76$ resonance from F_X in a wild-type complex is shown for reference. The Y-scale is offset arbitrarily. Sample conditions and spectrometer conditions are the same as in Figure 6 except that the field was scanned from 3200 to 3800 G and the temperature was 12 K.

in partial loss of the 10-μs flash-induced absorption transient attributed to the $P700^+ A_1^-$ back-reaction (Warren et al., 1993). We suggest that the interpolypeptide F_X cluster is rendered more susceptible to oxidative denaturation when cysteine-565 is replaced with a serine.

DISCUSSION

A photosystem I complex isolated from the C565S mutant of *Synechocystis* sp. PCC 6803 with dodecyl maltoside contains a population of [3Fe-4S] clusters and a population of [4Fe-4S] clusters in the F_X site. The latter represents the first example of a mixed-ligand iron–sulfur cluster in a protein with intersubunit coordination. It also shows that an interpolypeptide iron–sulfur protein is able to support a [3Fe-4S] cluster. Similar to the behavior of F_X, the [3Fe-4S] cluster undergoes photoreduction in the light at 15 K and charge recombination with $P700^+$ in subsequent darkness in about half of the reaction centers. However, unlike F_X, the [3Fe-4S] cluster undergoes reversible photoreduction in the presence of oxidized F_A and F_B. Since the [3Fe-4S] cluster can be reduced by dithionite at pH 6.5, its midpoint potential must be >–390 mV, and hence it is incapable on thermodynamic grounds of transferring its electron forward to the lower-potential clusters F_A (E_m, –530 mV) or F_B (E_m, –580 mV). The amount of P700 which undergoes reversible photooxidation at 15 K compared to that which undergoes irreversible charge separation indicates that the [3Fe-4S] cluster is present in only one-third to one-half of the C565S DM–PSI complexes.

This conclusion is supported by the finding that only half of the resident F_A and F_B clusters are photochemically reducible at room temperature. In those reaction centers in which P700 is coupled to irreversible F_A/F_B photoreduction, a new set of resonances are found with g-values of 2.015, 1.940, and 1.811 which are most probably derived from a $[4Fe\text{-}4S]^{2+,1+}$ cluster located in the F_X site. Similar to the behavior of wild-type F_X, the mixed-ligand [4Fe-4S] cluster, denoted F_X', appears to be capable of transferring an electron forward to oxidized F_A and F_B. Also similar to the behavior of wild-type F_X, the mixed-ligand F_X' cluster undergoes reversible photoreduction only in the presence of reduced F_A- and F_B-. Since the F_X' cluster cannot be reduced with dithionite at pH 10.0, it must have a midpoint potential <–600 mV, and hence it is capable of transferring its electron forward to the F_A and F_B clusters. It is not immediately apparent why there is a mixed population of $[3Fe\text{-}4S]^{1+,0}$ and $[4Fe\text{-}4S]^{2+,1+}$ clusters in the C565S complex. However, we failed to find any trace of [3Fe-4S] clusters in freshly-isolated thylakoid membranes from the C565S mutant (data not shown), implying that the fourth iron in the mixed-ligand [4Fe-4S] cluster may be susceptible to loss under certain conditions. We consider it likely that the C565S mutant incorporates a [4Fe-4S] cluster in vivo and that the cluster loses an iron in a minority of reaction centers during detergent treatment, producing a small population of [3Fe-4S] clusters.

We are not aware of any naturally-occurring [4Fe-4S] proteins which contain a serine ligand in lieu of a cysteine. However, site-directed mutations in *Escherichia coli* fumarate reductase subunit FrdB have been produced in which cysteines-204, -210, and -214 have been individually replaced by serine (Manodori et al., 1992). The mutations resulted in enzymes with negligible activity and associated loss of both [4Fe-4S] center 2 and [3Fe-4S] center 3. In contrast, site-directed mutations in *Escherichia coli* dimethyl-sulfoxide reductase subunit DmsB in which cysteine-102 was replaced by serine led to an assembled enzyme with altered activity (Rothery & Weiner, 1991). The oxidized enzyme showed an ESR spectrum with a peak at $g = 2.03$ (g_z) and a peak-trough at $g = 2.00$ (g_{xy}) characteristic of a $[3Fe\text{-}4S]^{1+}$ cluster. The

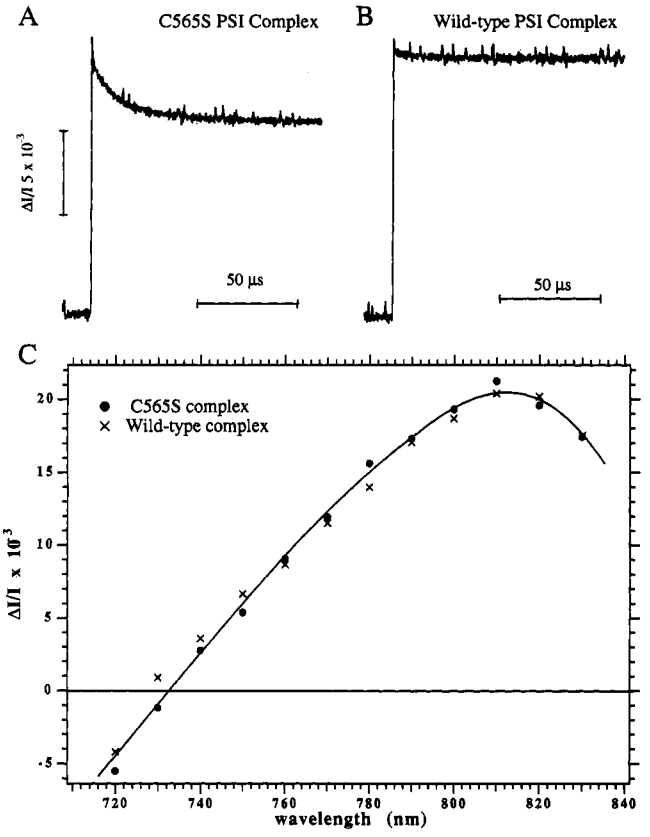

FIGURE 9: Absorption changes in the wild-type and C565S mutant complexes after a saturating flash. (A) C565S DM–PSI complex; (B) wild-type DM–PSII complex. All measurements were performed at 100 μg mL^{-1} chlorophyll *a* in 50 mM Tris-HCl buffer, pH 8.3, containing 1.7 mM ascorbate and 33 μM DCPIP. (C) Point-by-point difference spectrum from 720 to 830 nm of the wild-type DM–PSI complex (crosses) and the C565S DM–PSI complex (closed circles).

temperature dependencies, microwave power dependencies, and spin quantitations were consistent with the conversion of one of the [4Fe-4S] clusters into a [3Fe-4S] cluster.

There are known instances where a [4Fe-4S] cluster can lose an iron to form a [3Fe-4S] cluster and where a [3Fe-4S] cluster can incorporate a fourth iron to re-form a [4Fe-4S] cluster. The best example is aconitase, which has a [3Fe-4S] cluster due to the presence of only three appropriately-located cysteine ligands (Robbins & Stout, 1989). The $[3Fe\text{-}4S]^{1+,0}$ cluster has a high avidity for iron when in the reduced state; the iron displaces the water bound in the site, producing a $[4Fe\text{-}4S]^{2+,1+}$ cluster. The fourth iron in the [4Fe-4S] cluster probably has a water or hydroxyl as ligand [see Switzer (1989)], and the cluster has a high propensity for losing iron when in the oxidized state to re-form the [3Fe-4S] cluster. In *Desulfovibrio gigas* ferredoxin, FdII, either a [3Fe-4S] or a [4Fe-4S] cluster could be reconstituted depending on whether three Fe or four Fe were added per molecule of apoprotein (Moura et al., 1982). In a ferredoxin isolated from *Pyrococcus furiosus*, the second cysteine in the usual CxxCxxCxxxCP iron–sulfur binding motif is replaced by an aspartic acid (Connover et al., 1990). The single [4Fe-4S] cluster exists in both $S = {}^1/_2$ (20%) and $S = {}^3/_2$ (80%) spin states, and both forms show a midpoint potential of –365 mV. The cluster undergoes facile and quantitative interconversion between the [3Fe-4S] and [4Fe-4S] forms (Park et al., 1991). In ferredoxin isolated from *Desulfovibrio afracanus*, a [4Fe-4S] cluster and a [3Fe-4S] cluster are present; the latter correlates with the presence of an aspartic acid residue in place of a cysteine. The [4Fe-4S] cluster has a midpoint potential of –410 mV, but the [3Fe-4S] cluster has a relatively high potential of –140 mV (Armstrong et al., 1989). Only the [4Fe-4S] cluster exists in vivo although aerobic isolation induces partial degradation to the [3Fe-4S] form (George et al., 1989).

The site-directed mutants C565H and C565D did not accumulate photosystem I and failed to grow photoautotrophically (Smart et al., 1993), a finding consistent with the proposal that cysteine-565 does indeed coordinate F_X. The C565 mutant accumulates photosystem I, but the amount found is lower than the wild-type. This suggests that the photosystem I proteins are synthesized but they are rapidly degraded since the complex cannot stably form without F_X. It also implies that there is a greater turnover of the photosystem I reaction center, and hence a lower steady-state accumulation, in the cell. Perhaps the [4Fe-4S] cluster loses an iron at a constant rate because the cluster exists mostly in the oxidized state, and the resulting [3Fe-4S] cluster is recognized by the protein-turnover machinery as a damaged reaction center. It becomes degraded, but the rate of synthesis balances with the rate of degradation to produce a lower steady-state concentration of photosystem I. A site-directed change of the cysteine to aspartate, which leads to the in vitro incorporation of a [3Fe-4S] cluster in F_A and F_B of PsaC (Zhao et al., 1992), did not lead to the formation of a [3Fe-4S] cluster in F_X. This further suggests that those substitutions which do not allow formation of an intact [4Fe-4S] cluster produce a faulty photosystem I reaction center which is immediately recognized as damaged and becomes rapidly degraded. This could indicate that the F_X iron–sulfur cluster serves a structural as well as a functional role in photosystem I.

ACKNOWLEDGMENT

We are grateful to Dr. Neil Bowlby for isolating the DM–PSI complexes from the wild-type thylakoids and Dr. John Markwell for critically reading the manuscript. J.H.G. thanks Dr. Wolfgang Nitschke for valuable discussions on the ESR properties of interacting [4Fe-4S] clusters.

REFERENCES

Anderson, S. L., & McIntosh, L. (1991) *J. Bacteriol. 173*, 2761–2767.

Armstrong, F. A., George, S. J., Cammack, R., Hatchikian, E. C., & Thomson, A. J. (1989) *Biochem. J. 264*, 265–274.

Beinert, H., & Thomson, A. J. (1983) *Arch. Biochem. Biophys. 222*, 333–361.

Bryant, D. A. (1992) in *The Photosystems: Structure, Function, and Molecular Biology* (Barber, J., Ed.) pp 501–549, Elsevier, Amsterdam.

Chamorovsky, S. K., & Cammack, R. (1982) *Photobiochem. Photobiophys. 4*, 195–200.

Connover, R. C., Kowal, A. T., Fu, W., Park, J. B., Aono, S., Adams, M. W. W., & Johnson, M. K. (1990) *J. Biol. Chem. 265*, 8533–8541.

Crowder, M., & Bearden, A. (1983) *Biochim. Biophys. Acta 722*, 23–35.

Evans, M. C. W., & Heathcote, P. (1980) *Biochim. Biophys. Acta 590*, 89–96.

Evans, M. C. W., Sihra, C. K., & Cammack, R. (1976) *Biochem. J. 158*, 71–77.

Takahashi, Y., Goldschmidt-Clermont, M., Soen, S. Y., Franzen, L. G., & Rochaix, J. D. (1991) *EMBO J. 10*, 2033–2040.

George, S. J., Armstrong, F. A., Hatchikian, E. C., & Thomson, A. J. (1989) *Biochem. J. 264*, 275–284.

Georgiadis, M. M., Komiya, H., Chakrabarti, P., Woo, D., Kornuc, J. J., & Rees, D. C. (1992) *Science 257*, 1653–1659.

Golbeck, J. H. (1992) *Annu. Rev. Plant Physiol. Plant Mol. Biol. 43*, 293–324.

Golbeck, J. H., & Cornelius, J. M. (1986) *Biochim. Biophys. Acta 849*, 16–24.
Hausinger, R. P., & Howard, J. B. (1983) *J. Biol. Chem. 258*, 13486–13492.
Huynh, B. H., Moura, J. J. G., Moura, I., Kent, T. A., Legall, J., Xavier, A. V., & Münck, E. (1980) *J. Biol. Chem. 255*, 3242–3244.
Manodori, A., Cecchini, G., Schroder, I., Gunsalus, R. P., Werth, M. T., & Johnson, M. K. (1992) *Biochemistry 31*, 2703–2712.
Mathis, P., & Sétif, P. (1981) *Isr. J. Chem. 21*, 316–320.
Moura, J. J. G., Moura, I., Kent, T. A., Lipscomb, J. D., LeGall, J., Xavier, A. V., & Münck, E. (1982) *J. Biol. Chem. 257*, 6259–6267.
Norem, G. H., Boerner, R. J., & Barry, B. A. (1991) *Biochemistry 30*, 3943–3950.
Park, J. B., Fan, C. L., Hoffman, B. M., & Adams, M. W. W. (1991) *J. Biol. Chem. 266*, 19351–19356.
Parrett, K. G., Mehari, T., Warren, P., & Golbeck, J. H. (1989) *Biochim. Biophys. Acta 973*, 324–332.
Robbins, A. H., & Stout, G. H. (1989) *Proteins: Struct., Funct., Genet. 5*, 289–312.
Rothery, R. A., & Weiner, J. H. (1991) *Biochemistry 30*, 8296–8305.
Sétif, P., & Bottin, H. (1989) *Biochemistry 28*, 2689–2697.
Sétif, P., Mathis, P., & Vänngaard, T. (1984) *Biochim. Biophys. Acta 767*, 404–414.
Shuvalov, V. A., Klevanik, A. V., Sharkov, A. V., Kryukov, P. G., & Ke, B. (1979) *FEBS Lett. 107*, 313–316.
Smart, L. B., Anderson, S. L., & McIntosh, L. (1991) *EMBO J. 10*, 3289–3296.
Smart, L. B., Warren, P. V., Golbeck, J. H., & McIntosh, L. (1993) *Proc. Natl. Acad. Sci. U.S.A. 90*, 1132–1136.
Switzer, R. L. (1989) *BioFactors 2*, 77–86.
Warren, P. V., Golbeck, J. H., & Warden, J. T. (1993) *Biochemistry 32*, 849–857.
Zhao, J. D., Li, N., Warren, P. V., Golbeck, J. H., & Bryant, D. A. (1992) *Biochemistry 31*, 5093–5099.